Main-Group Chemistry

International Edition: DOI: 10.1002/anie.201601878
German Edition: DOI: 10.1002/ange.201601878

Isolation of Labile Pseudohalogen NSO Species

René Labbow, Dirk Michalik, Fabian Reiß, Axel Schulz, and Alexander Villinger*

Abstract: *A new synthetic approach enabled the generation of highly labile thionylimide, H–NSO, which was trapped by adduct formation with the bulky Lewis acid $B(C_6F_5)_3$ and fully characterized. For comparison, a series of different Me_3Si–NSO Lewis acid adducts were studied. Treatment of Me_3Si–NSO with the silylium ion $[Me_3Si]^+$ led to the formation of the hitherto unknown iminosulfonium ion $[Me_3Si–N{=}S–O–SiMe_3]^+$, which could be isolated and fully characterized as a salt in the presence of weakly coordinating carborate anions.*

Triatomic combinations of the elements carbon, nitrogen, and oxygen in anions (e.g., fulminate (CNO^-), azide (NNN^-), or cyanate (OCN^-)) as well as some heavier congeners (OCP^-, SCN^-, $SeCN^-$) are often referred to as linear pseudohalides.[1–3] Another triatomic combination is the bent thiazate NSO^- ion,[4] which is iso(valence)electronic to the bent pseudohalide NO_2^-. Essential criteria for pseudohalides (XYZ^-) are the existence of the free acid HXYZ and the pseudohalonium cation $[R–XYZ–R]^+$ (R = H, Me_3Si, or any alkyl or aryl substituent) as well as the formation of sparingly soluble heavy-metal salts.[5,6] Herein, we present a facile approach for the generation of pure H–NSO, its trapping by adduct formation, and the isolation of a salt bearing the highly labile, novel iminosulfonium ion $[R–N{=}S–O–R]^+$.

First attempts to generate H–NSO (**1**; thionylimide, also known as iminosulfane oxide, sulfinylamine, sulfoximine) date back to 1911, when Ephraim and Piotrowski treated $SOCl_2$ with NH_3 in the gas phase.[8] H–NSO is a colorless gas at ambient temperature but it can be condensed to a colorless liquid that freezes at −85 °C. Liquid H–NSO quickly polymerizes to a dark brown solid, polythionylimide $[(HNSO)_x]$.[9] Several theoretical[10–14] and experimental microwave studies[15–26] revealed a planar *cis*-HNSO species for the ground state (Scheme 1).[27] This structure can also be derived from C_{2v}-symmetric SO_2 by replacing one of the oxygen atoms by the divalent imide group (=NH). Like SO_2,[28] H–NSO was also found to have a small open-shell singlet biradical character as shown by CASSCF (complete active space self-consistent field) and NRT (natural resonance theory) computations (Scheme 1, see also the Supporting Information).[7]

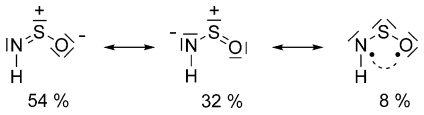

Scheme 1. Lewis formulae of *cis*-HNSO according to the NRT computations.[7]

Following our interest in pseudohalogen chemistry, we were intrigued by the idea to generate pure, highly labile H–NSO and to stabilize it in the solid state by adduct formation. As early as 1943, Schenk pointed out that the synthesis of H–NSO is hampered by the fact that condensed H–NSO (m.p. −85 °C) already polymerizes above −70 °C.[29] Therefore, the reaction of NH_3 and $SOCl_2$ needs to be carried out at low pressure and low temperatures. To avoid H–NSO polymerization, we envisaged to generate H–NSO in the presence of a strong and bulky Lewis acid (LA) such as $B(C_6F_5)_3$, which is known to stabilize reactive species.[30] Therefore, we adopted a different approach for H–NSO generation and adapted a procedure known from azide chemistry. In 1935, Günther, Meyer, and Müller-Skjøld had reported the synthesis of hydrazoic acid, $H–N_3$, in the reaction of fatty acids, such as palmitic acid, with metal azides.[31] Hence, in a first step, KNSO was heated with an excess of stearic acid (m.p. 69 °C) under vacuum. Once the stearic acid had melted, instant release of H–NSO gas was observed (Scheme 2). In a second step, the gas was transferred into a second attached flask containing a frozen solution of $B(C_6F_5)_3$ dissolved in CH_2Cl_2 at −196 °C in vacuo.[7] Pure H–NSO could thus be continuously condensed onto a frozen $B(C_6F_5)_3/CH_2Cl_2$ mixture. A slow increase in temperature to 20 °C resulted in the formation of a slightly turbid yellowish solution, from which colorless crystals suitable for single-crystal structure elucidation were obtained upon cooling to 5 °C overnight (Scheme 2). X-ray studies unequivocally confirmed the formation of the OS(H)N→$B(C_6F_5)_3$ adduct (**1**·$B(C_6F_5)_3$, Figure 1). The *cis*-HNSO moiety is preserved in the adduct while the $B(C_6F_5)_3$ group is attached to the N atom. Adduct **1**·$B(C_6F_5)_3$ is extremely

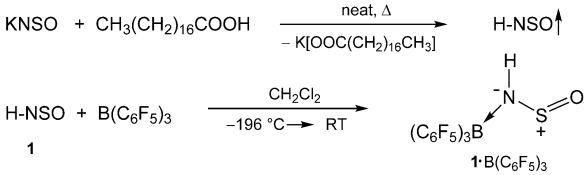

Scheme 2. Synthesis of *cis*-HNSO and trapping by adduct formation.[7]

[*] R. Labbow, Prof. Dr. A. Schulz, Dr. A. Villinger
Institut für Chemie, Universität Rostock
Albert-Einstein-Strasse 3a, 18059 Rostock (Deutschland)
E-mail: axel.schulz@uni-rostock.de
Homepage: http://www.schulz.chemie.uni-rostock.de/
Dr. D. Michalik, Dr. F. Reiß, Prof. Dr. A. Schulz
Leibniz-Institut für Katalyse e.V. an der Universität Rostock
Albert-Einstein-Strasse 29a, 18059 Rostock (Deutschland)

Supporting information (experimental and computational details) and the ORCID identification number(s) for the author(s) of this article can be found under http://dx.doi.org/10.1002/anie.201601878.

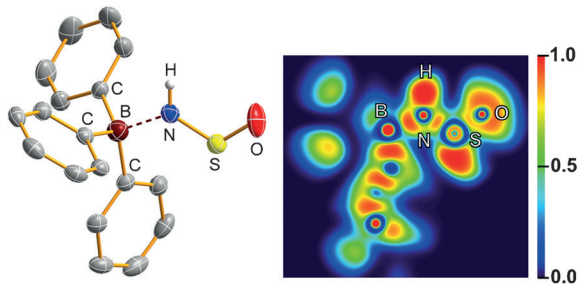

Figure 1. Left: ORTEP representation of the molecular structure of **1**·$B(C_6F_5)_3$ in the crystal. Thermal ellipsoids set at 50% probability (173 K). Fluorine atoms omitted for clarity. Right: Two-dimensional cross-section through the N–S–O plane of the electron localization function (ELF).

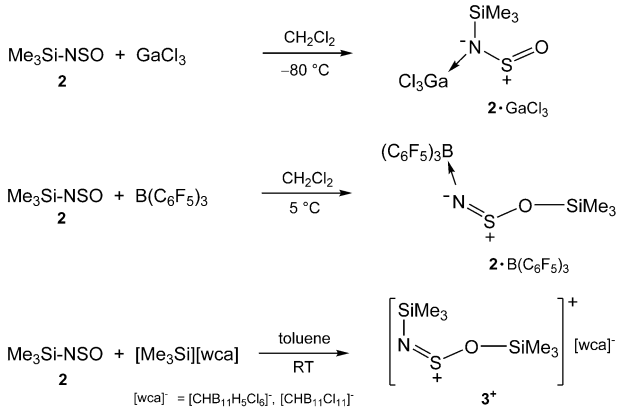

Scheme 3. Synthesis of Me_3Si–NSO adducts ($GaCl_3$, $B(C_6F_5)_3$) and $[Me_3Si{-}NSO{-}SiMe_3]^+$. wca = weakly coordinating anion.

moisture-sensitive and decomposes above 111 °C. $^1H,^{15}N$ HMBC (heteronuclear multiple bond correlation) 2D NMR studies of **1**·$B(C_6F_5)_3$ dissolved in $[D_8]$toluene revealed two cross peaks [$\delta(^1H) = 10.4/10.6$ ppm, $\delta(^{15}N) = -95/-106$ ppm, $^1J(^1H{-}^{15}N) = 65/70$ Hz), which is indicative of the co-existence of *cis* and *trans* isomers in solution (for HNSO: $\delta(^{14}N) = -73.8$ ppm, $\delta(^1H) = 9.86$ ppm, $^1J(^1H{-}^{14}N) = 65$ Hz; see the Supporting Information, Figures S7–S15). With temperature-dependent ^1H NMR spectroscopy, the *cis*/*trans* ratio in solution could be determined and the *cis*–*trans* isomer energy difference could be calculated, which amounts to 0.58 kcal mol^{-1} (Figures S18–S20), in accord with computations (in the gas phase: 2.1 kcal mol^{-1}; see Table 1). ^{11}B NMR experiments confirmed the presence of an intact **1**·$B(C_6F_5)_3$ species in solution as manifested by a strongly high-field-shifted resonance at $\delta(^{11}B) = -10$ ppm ($\delta = 59.8$ ppm for neat $B(C_6F_5)_3$ in $[D_8]$toluene), which is in accord with the range reported for four-coordinated boron atoms (−7 to −12 ppm when attached to an N atom in RCN).[32] We also tried to prepare the $GaCl_3$ adduct of H–NSO but failed to grow single crystals. However, in solution, we only observed OS(H)N→$GaCl_3$ (**1**·$GaCl_3$) with $\delta(^{14}N) = -112$ ppm and a broadened proton resonance at $\delta(^1H) = 8.32$ ppm (see the Supporting Information). Mews et al. have also reported on N coordination in a series of $[(CO)_5M{\leftarrow}N(H)SO][AsF_6]$ (M = Mn, Re) thionylimide transition-metal complexes on the basis of IR studies.[33]

To further increase the thermal stability of the thionylimide adducts, we also prepared adducts of Me_3Si–NSO (**2**), which can be regarded as a "large proton analogue" ($[Me_3Si]^+$) of H–NSO. As intended, upon substituting the H atom by Me_3Si, the thermal stability of R–NSO significantly increased; for example, Me_3Si–NSO can be distilled (b.p. 105–107 °C) without decomposition and is a stable liquid down to −80 °C. With Me_3Si–NSO in hand, it was now possible to study adducts with Lewis acids of various bulkiness and acid strength and compare these to H–NSO. Adducts of Me_3Si–NSO were easily formed upon treating Me_3Si–NSO with a LA (LA = $GaCl_3$, $B(C_6F_5)_3$) in CH_2Cl_2 (Scheme 3).[7] The synthesis of $[Me_3Si{-}NSO{-}SiMe_3]^+$ (**3**$^+$) salts was significantly more challenging and only successful when we used trimethylsilylium salts of *closo*-carborates of the type [Me_3Si][wca] ([wca]$^-$ = $[CHB_{11}H_5Cl_6]^-$, $[CHB_{11}Cl_{11}]^-$) in the reaction with Me_3Si–NSO (Scheme 3). Salts bearing the iminosulfonium ion $[Me_3Si{-}N{=}S{-}O{-}SiMe_3]^+$ were thus generated in moderate yields (25–30%). Highly dynamic behavior was observed for **3**$^+$ in solution (3 signals in the ^1H and ^{13}C spectra, and 2 in the ^{29}Si NMR spectrum), presumably indicating the isomerization process between the N,N- and N,O-bound species (see species A1 and B1 in Scheme 4). By contrast, only one species was detected for **2**·$GaCl_3$ and **2**·$B(C_6F_5)_3$. As expected in the latter two cases, the ^{29}Si (**2**·$GaCl_3$: $\delta = 26.0$; **2**·$B(C_6F_5)_3$: $\delta = 42.2$ ppm) and ^{14}N (**2**·$GaCl_3$: $\delta = -20$ ppm; **2**·$B(C_6F_5)_3$: not observed) resonances were strongly shifted downfield upon adduct formation (neat **2**: $\delta(^{29}Si) = 7.2$, $\delta(^{14}N) = -44$ ppm).

The single-crystal X-ray and NMR data of **2**·$GaCl_3$, **2**·$B(C_6F_5)_3$, and **3**$^+$ revealed different connectivities and structural parameters compared to **1**·$B(C_6F_5)_3$ (Figures 1, 2,

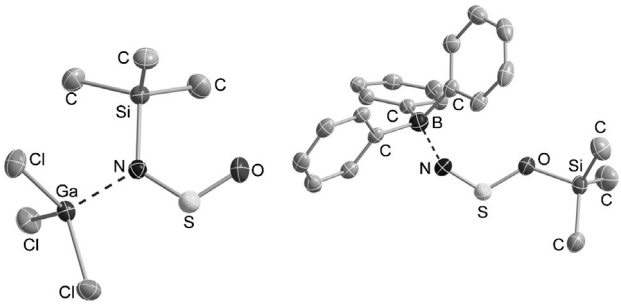

Figure 2. ORTEP representation of the molecular structure of **2**·$GaCl_3$ (left) and **2**·$B(C_6F_5)_3$ (right) in the crystal. Thermal ellipsoids set at 50% probability (173 K). Fluorine and hydrogen atoms omitted for clarity.

and 3). Whereas the small Lewis acid $GaCl_3$ adopts the same type of atomic arrangement (N,N-bound isomer A1; Scheme 4), with both the Me_3Si and $GaCl_3$ groups attached to the N atom, the larger Lewis acid $B(C_6F_5)_3$ triggers an isomerization process to the thermodynamically favored N,O-bound species (isomer C1), with the Me_3Si group now attached to the O atom and the $B(C_6F_5)_3$ group forming a donor–acceptor bond to the N atom. For **3**$^+$, a favorable

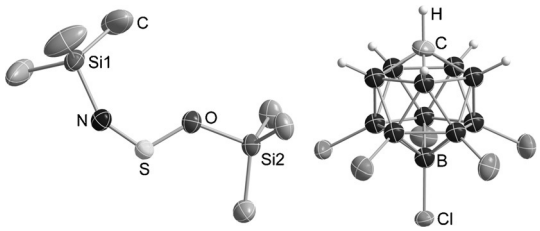

Figure 3. ORTEP representation of the molecular structure of **3**[$CHB_{11}H_5Cl_6$] in the crystal. Thermal ellipsoids set at 50% probability (173 K). Methyl hydrogen atoms omitted for clarity.

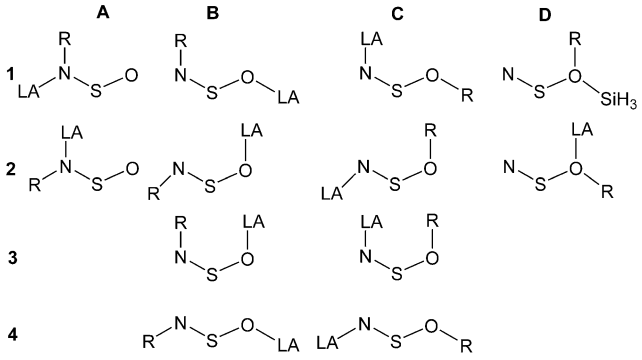

Scheme 4. Possible isomers of the R–NSO adducts (R = H, Me_3Si; LA = $GaCl_3$, $B(C_6F_5)_3$, or $[Me_3Si]^+$. Full PESs including the energies and the energetically unfavorable S-bound isomers are shown in Figures S50–S53.

N,O-bound species was also observed in accord with the situation reported for the pseudohalonium ion $[Me_3Si–NCO–SiMe_3]^+$.[5] To shed light on the structural diversity of these formal R–NSO·LA species (R = H, Me_3Si; LA = $GaCl_3$, $B(C_6F_5)_3$, and $[Me_3Si]^+$), we studied the potential energy surfaces (PESs) of all species in detail (Table 1, Figures S50–S53). First, in accordance with these theoretical data, the thermodynamically favored species always crystallized and were observed in the X-ray experiments. Aside from **2**·$B(C_6F_5)_3$, for all other considered species, the most stabile isomer always features the H or Me_3Si moiety attached at the N atom and *cis* to the O atom, thus allowing for a stabilizing intramolecular van der Waals interaction. Second, the PESs are rather flat with at least five isomers within 10 kcal mol^{-1}, clearly allowing for highly dynamical behavior in solution, especially in the presence of a Lewis acid, which can easily migrate along the NSO unit[10] or dissociate and bind to an adjacent atom.[30,34]

X-ray diffraction analysis (Figures 1–3) revealed an almost planar $R^1N(R^2)SO$ or $R^1–NSO–R^2$ skeleton as a main structural motif in all considered species always featuring a strongly bent NSO unit (angles of 114–117°, Table 2). Significant differences in the metrical parameters were found between the N,N- and N,O-bound species. Both N,N-bound adducts exhibit rather short S–O distances (**1**·$B(C_6F_5)_3$: 1.427(2) Å; **2**·$GaCl_3$: 1.439(2) Å) displaying double bond character (see Table 2; $\Sigma r_{cov.}(S{=}O) = 1.46$, $(S{\equiv}O) = 1.34$;[35] SO 1.481,[36] SO_2 1.43,[37] SO_3 1.419,[38] and $[SO_4]^{2-}$ 1.461 Å),[39] while the slightly longer S–N bonds (**1**·$B(C_6F_5)_3$: 1.5230(2) Å; **2**·$GaCl_3$: 1.540(2) Å) are in the range between a single and double bond ($\Sigma r_{cov}(N–S) = 1.73$, $(N{=}S) = 1.49$ Å).[35] On the contrary, the N,O-bound species **2**·$B(C_6F_5)_3$ and the salt **3**[$CH_5B_{11}Cl_6$] display very short N–S (**2**·$B(C_6F_5)_3$: 1.445(2); $\mathbf{3}^+$: 1.450(2) Å) and longer S–O (**2**·$B(C_6F_5)_3$: 1.556(2); $\mathbf{3}^+$: 1.531(2); $\Sigma r_{cov.}(S–O) = 1.70$, $(S{=}O) = 1.46$ Å)[35] distances. For comparison, an N–S bond length of 1.404(6) Å was found in the thiazylium salt $[NS][Sb_2F_{11}]$ at 121.5 K, which features an NS triple bond.[40] The structure of **3**[$CHB_{11}Cl_{11}$] as the toluene solvate could be determined, too; however, owing to the disorder of the NSO unit, the data are poor and do not allow a detailed discussion aside from confirming the connectivity (see Scheme S6 and Table S8).

The Ga–N donor–acceptor bond in **2**·$GaCl_3$ with 2.003(1) Å is in the expected range[41] (1.965(2) Å in $Me_3Si–N{=}S{=}N–SiMe_3{\cdot}GaCl_3$).[42] A closer look at the B–N donor–acceptor bond lengths revealed slightly elongated distances in **1**·$B(C_6F_5)_3$, with 1.624(3) Å compared to 1.598(2) Å in

Table 1: Relative energies [kcal mol^{-1}] of the isomers of **1**, **2**, and $\mathbf{3}^+$ (see Scheme 4) computed at the pbe0/aug-cc-pwCVDZ level of theory.

Isomer	**1**·$B(C_6F_5)_3$	**2**·$B(C_6F_5)_3$	**2**·$GaCl_3$	$\mathbf{3}^+$[a]
A1	**0.0**[b]	4.9	**0.0**	4.0
A2	2.1[b]	6.1	3.6	4.0
B1	9.4	0.4	–[c]	**0.0**
B2	14.1	3.7	–[c]	0.7
B3	9.1	–[c]	3.7	–[c]
B4	12.6	4.3	5.8	2.3
C1	17.1	**0.0**	–[c]	**0.0**
C2	15.4	1.0	–[c]	0.7
C3	10.9	–[c]	–[c]	–[c]
C4	18.5	–[c]	10.9	2.3
D1	23.7	19.8	15.7	20.1
D2	27.2	64.8	–[c]	20.1

[a] A1/A2, B1/C1, B2/C2, B3/C3, and B4/C4 are identical as R = LA. [b] An energy gap of 0.58 kcal mol^{-1} between A1 (*cis*) and A2 (*trans*) was determined by temperature-variable ^{1}H NMR spectroscopy in the liquid state (see Figures S18–S20). [c] Not a stable isomer (with zero imaginary frequencies).

Table 2: Selected structural data of NSO compounds.

Compound	N–S [Å]	S–O [Å]	N-S-O [°]
1[a]	1.5123	1.4513	120.41
2[b]	1.508(5)	1.444(4)	122(1)
K[NSO][c]	1.442(5)[d]	1.442(5)[d]	123.7(5)
Rb[NSO][c]	1.465(4)[d]	1.465(4)[d]	121.1(4)
$[Me_4N][NSO]$[e]	1.431(8)[d]	1.438 (7)[d]	126.8(4)
1·$B(C_6F_5)_3$	1.530(2)	1.427(2)	114.3(2)
2·$GaCl_3$	1.540(2)	1.439(2)	114.59(6)
2·$B(C_6F_5)_3$[f]	1.445(2)	1.556(2)	117.08(8)
3[$CH_5B_{11}Cl_6$]	1.450(2)	1.531(2)	115.2(2)

[a] Microwave spectroscopy, taken from Ref. [43]. [b] Electron diffraction, taken from Ref. [44]. [c] Powder X-ray diffraction, taken from Ref. [45]. [d] Impossible to distinguish between N and O. [e] Taken from Ref. [46]. [f] Values for α-**2**·$B(C_6F_5)_3$ with the space group $P\bar{1}$; a β-phase with the space group $P2_1/n$ also exists (see the Supporting Information).

$2{\cdot}B(C_6F_5)_3$ (1.616(3) Å in $CH_3CN{\cdot}B(C_6F_5)_3$,[32] $\Sigma r_{cov}(B{-}N) = 1.56$ Å),[35] which can be attributed to the larger steric hindrance in $1{\cdot}B(C_6F_5)_3$.

To explain the structural peculiarity with respect to the short NS and SO bonds, the electronic structure was studied by means of NBO (natural bond orbital), NRT, MO (molecular orbital), and ELF calculations. We first computed the parent species NSO^-, H–NSO, $[H_2NSO]^+$, and $[HNSOH]^+$ (Tables S18 and S19; Figure 4). According to

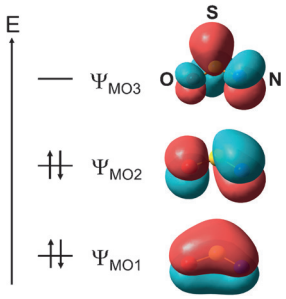

Figure 4. MO diagram of the four-electron-three-center π system in NSO^-.

the MO calculations, the most prominent electronic feature is the presence of a four-electron-three-center π system in all of these species (shown for NSO^- in Figure 4; for all others, see Table S18).[11] The lowest MO1 is always bonding between NS and SO, the second one (MO2) is NS bonding and SO antibonding, while the third one is the entirely antibonding combination and always represents the LUMO (lowest unoccupied molecular orbital; the exact MO coefficients are listed in Table S19). The net effect of the two occupied valence MOs is a strong NS π bond (with a total bond order close to two) but a very weak SO π bond (with a total bond order close to one). This can be expressed by the dominant Lewis-type representation $N^{(-)}{=}S^{(+)}{-}O^{(-)}$, which is in good agreement with the NRT and NBO picture (e.g., see Scheme 1 or Figure S58/S59). However, this description only holds true for NSO^-, R–NSO, R–NSO–LA (e.g., $2{\cdot}B(C_6F_5)_3$), and $[R{-}NSO{-}R]^+$ (e.g., $\mathbf{3}^+$) species; that is, only for species with only one ligand attached to the nitrogen atom, shorter NS and longer SO bonds are observed. In all N,N-bound species, the character of the four-electron-three-center bond changes; in particular, MO2 is now nonbonding between NS and SO as the coefficient of the p_z atomic orbitals at the S atom is essentially zero (Table S19). As the coefficients at the O atom are larger than those at the N atom in MO1, a stronger SO (weaker NS) π bond is observed, which is in accord with the NRT and NBO computations as well as the experimentally found longer NS and shorter SO bonds (e.g., in $1{\cdot}B(C_6F_5)_3$ and $2{\cdot}GaCl_3$). In these cases, the most important Lewis structure, $[R(LA)N^{(-)}{-}S^{(+)}{=}O]$, features one SO double and one NS single bond. NBO/NRT/ELF data of all considered NSO species indicate strongly polar NS and very strongly polar SO bonds as well as a well-localized lone pair at the S atom (Tables S12–S17, Figure S55). As can be seen from the ELF data for $1{\cdot}B(C_6F_5)_3$ (Figure 1), for example, the electron density of the donor–acceptor bond is localized in the proximity of the nitrogen atom, and the charge transfer, derived from the NPA charges, amounts to 0.36 e (0.38 e in $2{\cdot}B(C_6F_5)_3$) and 0.16 e in $2{\cdot}GaCl_3$; NPA = natural population analysis).

In summary, we have developed a facile synthetic method to generate the highly labile H–NSO adduct, which has also been fully characterized. Furthermore, adducts of the heavier congener Me_3Si–NSO along with hitherto unknown N,O-iminosulfonium $[Me_3Si{-}NSO{-}SiMe_3]^+$ salts have been isolated and characterized, thus confirming that the triatomic NSO group can be viewed as a pseudohalogen. In view of the isoelectronic relationship between $[Me_3SiNSOSiMe_3]^+$ and $Me_3SiNSNSiMe_3$, the former compound is a potentially versatile reagent for the transfer of an NSO^+ unit in metathesis or cyclocondensation reactions. With respect to the different charges, it could be considered as complementary to salts of the NSO^- anion in such applications.

Acknowledgments

We thank Jonas Bresien (University of Rostock) and Dr. Jens Krüger (University of Tübingen) for help with software- and network-related problems. Prof. Dr. Risto Laitinen (University of Oulu) and both reviewers are gratefully acknowledged for helpful advice.

Keywords: adducts · pseudohalogens · silylium cations · sulfinyl imines · thionyl imides

How to cite: *Angew. Chem. Int. Ed.* **2016**, *55*, 7680–7684
Angew. Chem. **2016**, *128*, 7811–7815

[1] L. Birckenbach, K. Kellermann, *Chem. Ber.* **1925**, *58*, 786–794.
[2] H. Brand, A. Schulz, A. Villinger, *Z. Anorg. Allg. Chem.* **2007**, *633*, 22–35.
[3] V. V. Stopenko, A. M. Golub, H. Köhler, *Chemistry of Pseudohalides*, Elsevier, Amsterdam, **1986**.
[4] D. A. Armitage, J. C. Brand, *J. Chem. Soc. Chem. Commun.* **1979**, 1078–1079.
[5] A. Schulz, A. Villinger, *Chem. Eur. J.* **2010**, *16*, 7276–7281.
[6] M. Lehmann, A. Schulz, A. Villinger, *Angew. Chem. Int. Ed.* **2009**, *48*, 7444–7447; *Angew. Chem.* **2009**, *121*, 7580–7583.
[7] The Supporting Information contains a detailed description of all experiments and computations as well as all spectra.
[8] F. Ephraim, H. Piotrowski, *Chem. Ber.* **1911**, *44*, 379–386.
[9] M. Becke-Goehring, R. Schwarz, W. Spiess, *Z. Anorg. Allg. Chem.* **1958**, *293*, 294–301.
[10] P. V. Bharatam, Amita, D. Kaur, P. S. Kumar, *Int. J. Quantum Chem.* **2006**, *106*, 1237–1249.
[11] C. Ehrhardt, R. Ahlrichs, *Chem. Phys.* **1986**, *108*, 417–428.
[12] N. H. Morgon, H. V. Linnert, J. M. Riveros, *J. Phys. Chem.* **1995**, *99*, 11667–11672.
[13] A. G. Turner, *Inorg. Chim. Acta* **1984**, *84*, 85–87.
[14] M. Méndez, J. S. Francisco, D. A. Dixon, *Chem. Eur. J.* **2014**, *20*, 10231–10235.
[15] M. J. Almond, A. J. Downs, T. L. Jeffery, *Polyhedron* **1988**, *7*, 629–634.
[16] R. L. DeKock, M. S. Haddad, *Inorg. Chem.* **1977**, *16*, 216–217.
[17] A. Haas, U. Fleischer, M. Mätschke, V. Staemmler, *Z. Anorg. Allg. Chem.* **1999**, *625*, 681–692.
[18] D.-L. Joo, D. J. Clouthier, *J. Chem. Phys.* **1996**, *104*, 8852–8856.

[19] M. Nonella, J. R. Huber, T. K. Ha, *J. Phys. Chem.* **1987**, *91*, 5203 – 5209.
[20] L. Puskar, E. G. Robertson, D. McNaughton, *J. Mol. Spectrosc.* **2006**, *240*, 244 – 250.
[21] H. Richert, *Z. Anorg. Allg. Chem.* **1961**, *309*, 171 – 180.
[22] T. Hata, S. Kinumaki, *Nature* **1964**, *203*, 1378 – 1379.
[23] D. M. Byler, H. Susi, *J. Mol. Struct.* **1981**, *77*, 25 – 36.
[24] R. P. Müller, M. Nonella, P. Russegger, J. R. Huber, *Chem. Phys.* **1984**, *87*, 351 – 361.
[25] A. D. Borgo, G. Lonardo, F. Scappini, A. Trombetti, *Chem. Phys. Lett.* **1979**, *63*, 115 – 118.
[26] N. Heineking, M. C. L. Gerry, *J. Mol. Spectrosc.* **1993**, *158*, 62 – 68.
[27] J. Demaison, L. Margulès, J. E. Boggs, H. D. Rudolph, *Struct. Chem.* **2001**, *12*, 1 – 13.
[28] E. Miliordos, S. S. Xantheas, *J. Am. Chem. Soc.* **2014**, *136*, 2808 – 2817.
[29] P. W. Schenk, *Chem. Ber.* **1942**, *75*, 94 – 99.
[30] F. Reiß, A. Schulz, A. Villinger, *Chem. Eur. J.* **2014**, *20*, 11800 – 11811.
[31] P. Günther, R. Meyer, F. Müller-Skjøld, *Z. Phys. Chem. A* **1935**, *175*, 154 – 169.
[32] A. Bernsdorf, H. Brand, R. Hellmann, M. Köckerling, A. Schulz, A. Villinger, K. Voss, *J. Am. Chem. Soc.* **2009**, *131*, 8958 – 8970.
[33] G. Hartmann, R. Hoppenheit, R. Mews, *Inorg. Chim. Acta* **1983**, *76*, L201 – L202.
[34] W. Baumann, D. Michalik, F. Reiß, A. Schulz, A. Villinger, *Angew. Chem. Int. Ed.* **2014**, *53*, 3250 – 3253; *Angew. Chem.* **2014**, *126*, 3314 – 3318.
[35] N. Wiberg, A. F. Holleman, *Lehrbuch der Anorgischen Chemie*, Walter De Gruyter, Berlin, New York, **2007**, Appendix V.
[36] E. Tiemann, *J. Phys. Chem. Ref. Data* **1974**, *3*, 259 – 268.
[37] V. Schomaker, D. P. Stevenson, *J. Am. Chem. Soc.* **1940**, *62*, 1270 – 1272.
[38] A. Kaldor, A. G. Maki, *J. Mol. Struct.* **1973**, *15*, 123 – 130.
[39] M. Malchus, M. Jansen, *Acta Crystallogr. Sect. B* **1998**, *54*, 494 – 502.
[40] W. Clegg, O. Glemser, K. Harms, G. Hartmann, R. Mews, M. Noltemeyer, G. M. Sheldrick, *Acta Crystallogr. Sect. B* **1981**, *37*, 548 – 552.
[41] E. I. Davydova, T. N. Sevastianova, A. V. Suvorov, A. Y. Timoshkin, *Coord. Chem. Rev.* **2010**, *254*, 2031 – 2077.
[42] C. Hubrich, A. Schulz, A. Villinger, *Z. Anorg. Allg. Chem.* **2007**, *633*, 2362 – 2366.
[43] M. Carlotti, G. Di Lonardo, G. Galloni, A. Trombetti, *J. Mol. Spectrosc.* **1980**, *84*, 155 – 161.
[44] K. I. Gobbato, C. O. D. Védova, H. Oberhammer, *J. Mol. Struct.* **1995**, *350*, 227 – 231.
[45] S. Mann, M. Jansen, *Z. Anorg. Allg. Chem.* **1995**, *621*, 153 – 158.
[46] S. Mann, M. Jansen, *Z. Naturforsch. B* **1994**, *49b*, 1503 – 1506.

Received: February 23, 2016
Published online: April 13, 2016

